EXPLAINING DIFFERENTIAL SOURCES OF ZOONOTIC PATHOGENS IN INTENSIVELY-FARMED CATCHMENTS USING KINEMATIC WAVES

Graham B. McBride
Principal Scientist, NIWA (National Institute of Water and Atmospheric Research), Hamilton

ABSTRACT

Aquatic microbiological surveys in streams draining intensively farmed catchments can, during flood events, indicate differential time-concentration patterns between a bacterial health-risk indicator (*E. coli*) and a major zoonotic bacterial pathogen that it seeks to indicate—*Campylobacter*. For example, the indicator's peak concentration at a monitoring station can arrive ahead of the flood peak (i.e., the pollutograph *leads* the hydrograph), whereas the peak pathogen concentration arrives *with* the flood peak (in which case the pollutograph and hydrograph peaks *coincide*). Observations for other bacteria have indicated cases where the *E. coli* pollutograph *lags* the hydrograph. These observations have generated the hypothesis that such behaviour reflects the possibility of there being three different possible (predominant) sources of pathogens in the floodwater: (i) by sediment entrainment, (ii) via local land runoff, or (iii) from upstream releases (e.g., from dams, inflows, or upstream floods). A general theory for contaminants in idealized stream floods has been developed, considering all three sources, based on kinematic wave theory. It can explain the observed differential time-concentration patterns. The calculation procedures and associated results are intended to inform public policy, by identifying predominant pathogen sources and therefore helping to focus attention on the important delivery mechanisms. This will better inform quantitative health risk assessments for downstream water users (recreational uses, water supplies, food production and processing industries).

KEYWORDS

Pathogens, *Campylobacter*, *E. coli*, streams, kinematic waves, runoff, sediments, numerical models.

1. INTRODUCTION

Consider two *local* mechanisms of microbial (bacterial) transport through stream systems during rainfall. Firstly, rain water flowing overland toward stream banks can entrain bacteria from previously deposited faecal material (Nagels *et al.* 2002, Muirhead *et al*. 2004). It seems that this is generally occurs. Secondly, enhanced stream velocity during floods drives entrainment of any faecal material in the stream sediments and on its banks. This seems not to generally occur, at least in the case of the troublesome bacterium *Campylobacter*, an important zoonotic pathogen.[1] This is because the sediments may be depauperate in the pathogen yet rich in its *E. coli* indicator, as has been found in sediment surveys in a Waikato stream draining intensive pastoral agriculture (Snowshill 2007).[2]

This observation provides the motivation for studying the differential timing of peaks of *Campylobacter* versus *E. coli* during storm flood events, as shown in Figure 1, using kinematic waves.

[1] This pathogen is of considerable public concern, given the high rate of reporting of its zoonosis—campylobacteriosis. This disease has been reported at up to 400 cases per 100,000 persons per annum (Till & McBride 2004). It is the subject of a major modelling research effort (Lake *et al*. 2007), which has funded much of the work reported herein. Animals are its major "reservoir", and so identifying effective intervention strategies to minimise its transmission to humans includes consideration of its transport characteristics over land and in freshwater streams.

[2] This result was actually predicted by Donnison *et al*. (2006).

Figure 1:Concentrations of *E. coli* (Colilert®) and *Campylobacter* (MPN) measured on autosamples taken over a flood event in the Toenepi Stream, Waikato in September 2005, along with flow and turbidity. Peak microbial concentrations are annotated by ovals. Data: Donnison *et al.* 2006, Lydiard & Davies-Colley 2006

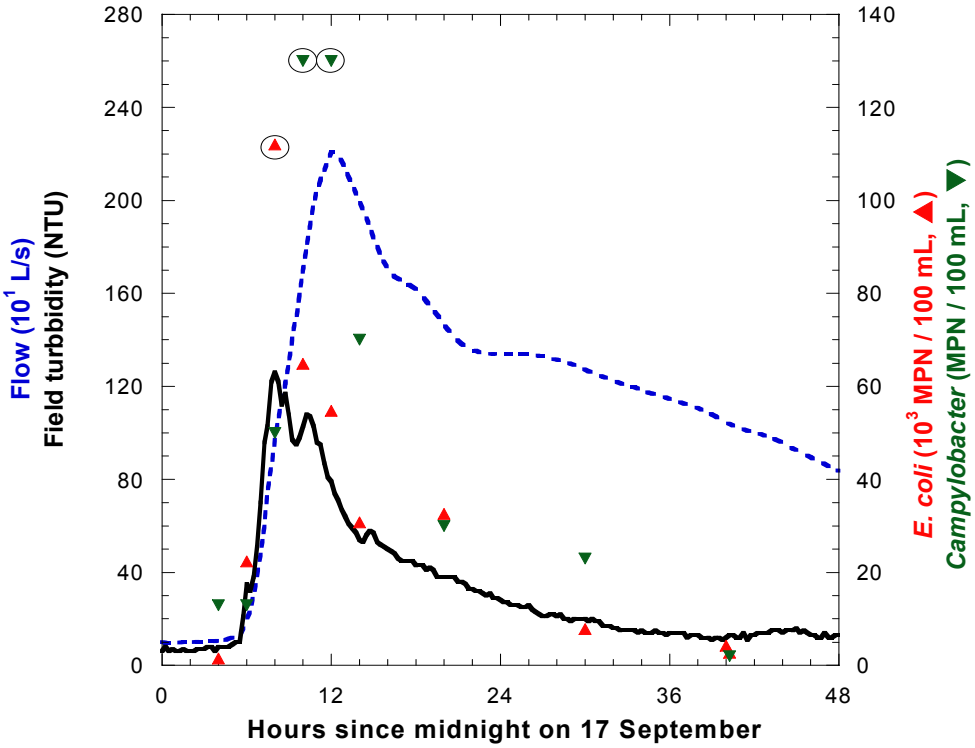

The appropriateness of kinematic wave theory, at least for smaller steeper streams, has been endorsed by Li *et al*. 1975 and by Krein & De Sutter 2001) who observed that "there is a lag in the arrival of the flood water behind the rise in stage". Its huge advantage, as we shall see, is to replace a complex momentum balance with a simple power law.

More generally, other observations (pers. comm. Dr Rob Davies-Colley, NIWA, Hamilton) have shown that a microbial stream "pollutograph" can lag, lead or be in harmony with the stream's hydrograph.

2. CONCEPTUAL MODEL

Following a speculation made by Wilkinson *et al*. (2006), we seek to mimic such differential peak timing behaviour using a mathematical model based on kinematic wave theory, described in some detail by McBride & Mittinty 2007. The development was assisted by a clear exposition of the possible use of kinematic waves for contaminant hydrology by Chapra (1997). It has three main equations, for: (i) flow hydraulics, (ii) concentration of bacteria in the stream sediments, and (iii) concentration of bacteria in the stream water. We do so for an idealized situation in which we consider a stream segment with a dam as its upstream boundary, so that its upstream boundary flow (Q_b) is constant, even during rainfall. Our interest lies in monitoring and predicting the pollutograph at a downstream monitoring station.

Rainfall commences at time zero, giving rise to a uniform rate of lateral inflow along the stream length, in which there is no tributary inflow. At the end of the event the lateral inflow ceases abruptly. Concentrations of bacteria in the lateral inflow can vary with time. There is a known concentration of bacteria in the sediments at the start of the event.

Major assumptions concerning mechanisms operating are as follows.

2.1 ASSUMPTIONS ABOUT LATERAL INFLOW

The first runoff flush can be expected to result from higher bacteria entrainment rates than later in the storm, as stores become depleted. However, the lateral land distance over which the former entrainment has occurred will be smaller than that occurring later in the storm when the entrainment rate *at a point* is lower, but the distance over which entrainment occurs is longer—compensating for the higher point-wise entrainment rate. Accordingly, during the constant overland flow period the delivery of bacteria to the stream could possibly be taken as zero-order (constant) during the runoff period; that is,

$$M_l = rC_l \tag{1}$$

where M_l [# T^{-1} L^{-1}] is the land-derived bacteria delivery rate per unit channel length ("#" denotes numbers of bacteria), r [L^2 T^{-1}] (a constant) is the overland flow rate per unit channel length, and C_l [# L^{-3}] is the concentration of bacteria in the lateral inflow.

2.2 ASSUMPTIONS ABOUT ENTRAINMENT

We assume that the finiteness of the sediment microbial store demands that the bacterial entrainment rate is first-order and proportional to the remaining store after entrainment has commenced. Also, following Valentine & Wood (1979) (see also Rutherford 1994), that rate is taken to be proportional to the floodflow velocity excess, that is,

$$M_s = e_s\left(\frac{U - U_b}{U_b}\right)S \tag{2}$$

where M_s [# T^{-1} L^{-1}] is the delivery rate of entrained bacteria per unit channel length, e_s [T^{-1}] is the stream entrainment coefficient, U [L T^{-1}] is the cross-section average flow velocity (with value U_b at baseflow, from the dam outlet), and S [# L^{-1}] is the store of bacteria in the stream sediments and banks per unit channel length. Entrainment occurs when $U > U_b$ but there is deposition when $U < U_b$, as seems reasonable.

2.3 WHY ANALYSE SUCH A SIMPLE CASE?

We advance three reasons.

Firstly, this approach involves a novel application of kinematic wave theory—its application to surface water contamination is rare (Singh 2002). It therefore seems prudent to examine such a simple case, to help identify any problems in mathematical formulation of the problem and the use of associated equation solution techniques.

Secondly, the equation solution procedures generally require the use of approximate numerical methods, because analytical solutions have not been found. This makes "benchmarking" of the solution procedure difficult. However, we have obtained an analytical solution for one simple case (lateral inflow to a wide channel with positive baseflow, as summarised in the Appendix), which provides for some concrete benchmarking.

Finally, simple cases such as proposed can actually provide more *general insight* into contaminant hydrology than is the case for much more elaborate models, which tend to focus on *particular cases*.

2.4 SOLVING THE EQUATIONS

In the initial formulation of the problem by McBride & Mittinty (2007), and following Chapra (1997), an explicit numerical scheme was used. This has the advantage of relative simplicity (compared with an implicit scheme), but also has a drawback in that it isn't fully mass-conserving, and introduces "numerical dispersion" in which waves tend to be artificially smeared out. The mathematics of rather more elaborate implicit numerical schemes has been developed, and is in the process of implementation. This has been based on the attractive "four-point Preissman" scheme (Liggett & Cunge 1975, Abbott & Basco 1989, Martin & McCutcheon 1999). Its main attraction is that its computational molecule doesn't involve any nodes outside a particular grid cell which, on physical grounds, is only needed in the presence of second-order diffusion terms.

Herein, we mostly repeat the explicit approach taken in McBride & Mittinty (2007).

The algorithms were developed in Microsoft Excel-Visual Basic.

3. TRANSPORT EQUATIONS

Here we essentially repeat the development reported by McBride & Mittinty (2007), extending the model to include bacterial inactivation (which occurs principally by UV radiation).

3.1 CONTINUITY (WATER BALANCE) EQUATION

Application of mass conservation principles leads to the well-known equation

$$\frac{\partial A}{\partial t}+\frac{\partial Q}{\partial x}=r \tag{3}$$

where A [L^2] is the stream cross-section area, Q [$L^3\ T^{-1}$] is the stream discharge (with baseflow value Q_b, at the dam), x [L] is distance along the channel, and t [T] is time since flood commencement—r has been defined above. Each term in Eq. (3) has units [$L^2\ T^{-1}$].

Following Chapra (1997), we adopt the key assumption of kinematic wave theory—that the discharge is a function of depth alone—and use the Manning equation[3]

$$Q=\frac{\rho}{n}\frac{A^{5/3}}{P^{2/3}}\sqrt{\theta} \tag{4}$$

where θ [dimensionless] is the channel slope, P [L] is the wetted perimeter, n [dimensionless] is the Manning roughness coefficient and ρ is the units adjustment factor.[4] This equation can be solved for the fundamental kinematic wave equation (which obviates the need to develop a much more complex momentum balance equation)

$$A=\alpha Q^{\beta} \tag{5}$$

where

$$\beta=\frac{3}{5}\ \text{ and }\ \alpha=\left(\frac{nP^{2/3}}{\sqrt{\theta}}\right)^{3/5} \tag{6}$$

demonstrating that α is variable, not constant (because the wetted perimeter changes with discharge). However, the value of α becomes nearly constant for a rectangular channel much wider than it is deep—because we then have $P \approx B_0$, where B_0 [L] is the channel width. The value of α is then

$$\alpha\approx\left(\frac{nB_0^{2/3}}{\sqrt{\theta}}\right)^{3/5} \tag{7}$$

Differentiating Eq. (5) with respect to time and substituting the result into Eq. (3) we have the kinematic wave equation (Chapra 1997) augmented by lateral inflow

$$\frac{\partial Q}{\partial x}+\alpha\beta Q^{\beta-1}\frac{\partial Q}{\partial t}=r \tag{8}$$

By substituting explicit forward-time/backward-space differences, Eq. (8) can be represented by the approximate difference equation

$$\frac{Q_i^n-Q_{i-1}^n}{\Delta x}+\alpha\beta\left(Q_i^n\right)^{\beta-1}\left(\frac{Q_i^{n+1}-Q_i^n}{\Delta t}\right)\approx r \tag{9}$$

---

[3] According to Henderson (1966), Flamant (in 1891) wrongly attributed this equation to Manning. He noted that it was derived by Gauckler in 1868 and Hagen in 1881. In Europe the equation is often known as the Gauckler-Strickler equation, or just Strickler equation, although Strickler's contribution was made in the 1920s!

[4] The value of n is calibrated such that the numerical value of ρ is 1 in metres-second units (i.e., $\rho \equiv 1\ m^{1/3}\ s^{-1}$). In contrast, were we to use the similarly popular Chézy resistance equation (in which case $\beta = 2/3$), the value of ρ is 1 *in feet-second units* (i.e., $\rho \equiv 1\ ft^{1/2}\ s^{-1}$). Chow (1959, sec. 5-4) notes that even though a French engineer (Chézy) developed this equation (in 1769) it has become customary to report it in English units.

where, for example, $Q_i^n = Q(i\Delta x, n\Delta t)$, etc., such that i = 1, 2,… $i_{\max}$ and n = 0, 1, 2,… $n_{\max}$ (i counts downstream distance steps; n counts time steps). This can be simply solved for the unknown stream discharge

$$Q_i^{n+1} \approx Q_i^n + (U_c)_i^n \left(\frac{Q_{i-1}^n - Q_i^n}{\Delta x} + r \right) \Delta t \tag{10}$$

in which

$$U_c = \frac{Q^{1-\beta}}{\alpha\beta} \tag{11}$$

is the celerity of the kinematic wave [L T^{-1}]. This is always greater than the cross-section average velocity of the stream water (Chapra 1997), defined by $U = Q/A$.

3.2 SEDIMENT BACTERIA EQUATION

We assume that the bacteria (and sediment) in the stream bed do not move downstream whilst in the bed, but can be entrained into the water column and so be convected downstream in the water (so there is no $\partial/\partial x$ term). In that case we simply have

$$\frac{\partial S}{\partial t} = -e_s \mu S : \ \mu = \frac{U - U_b}{U_b} \tag{12}$$

where all variables are as defined earlier. Each term in Eq. (12) has units [# L^{-1} T^{-1}]. Using backward-time differencing for the temporal derivative, the approximating difference equation is

$$S_i^{n+1} \approx \left(1 - e_s \mu_i^n \Delta t\right) S_i^n \tag{13}$$

The initial density of bacteria in the bed, S_0 [# L^{-1}], is taken to be constant down the channel. For input to the model we typically have data for the number of bacteria per unit area of stream bed (s). This is simply related to the S variable by $S = sB_0$.

3.3 AQUATIC BACTERIA EQUATION

From mass conservation principles we obtain

$$\frac{\partial AC}{\partial t} + \frac{\partial QC}{\partial x} = rC_l + e_s \mu S - kAC \tag{14}$$

where $C(x, t)$ [# L^3] is the concentration of bacteria in the stream water and k is the bacteria inactivation coefficient—omitted from the McBride & Mittinty (2007) formulation. All other variables have already been defined. Each term in Eq. (14) has units [# L^{-1} T^{-1}]. Using backward-time differencing for the temporal derivative and defining a segment volume as $V = A\Delta x$, the approximating difference equation is

$$\frac{(VC)_i^{n+1} - (VC)_i^n}{\Delta t} \approx (QC)_{i-1}^n - (QC)_i^n + \left(rC_l + e_s \mu_i^n S_i^n\right) \Delta x \tag{15}$$

Now, noting that the lateral inflow adds a volume of $r\Delta x\Delta t$ to each segment during each time step, we can write the term $(VC)_i^{n+1}$ as

$$(VC)_i^{n+1} = \left[V_i^n + \left(Q_{i-1}^n - Q_i^n + r\Delta x\right)\Delta t\right] C_i^{n+1} \tag{16}$$

Substitution into Eq. (15) gives

$$C_i^{n+1} \approx \frac{V_i^n C_i^n + \left[Q_{i-1}^n C_{i-1}^n - Q_i^n C_i^n + \left(rC_l + e_s \mu_i^n S_i^n\right) \Delta x\right] \Delta t}{V_i^n + \left(Q_{i-1}^n - Q_i^n + r\Delta x\right) \Delta t} \tag{17}$$

The numerator represents the mass in the segment i at the previous time step, while the denominator represents its volume.

`

4 INDICATIVE RESULTS

All results shown are direct copies of graphs produced within the Visual Basic environment, with dynamic headers echoing key input values. They are intended to be indicative only, as this is a work-in-progress.

In Figure 2 we show predictions of the downstream hydrograph for both Cases I and II (as defined in the Appendix). Case I occurs when the inflow duration (t_0) exceeds the catchment's "time of concentration" (t_s), and vice versa for Case II.[5]

Figure 2: Predictions of stream discharge for Cases I and II [6]using both explicit and implicit schemes, and comparing wide channel solutions with the analytical solution

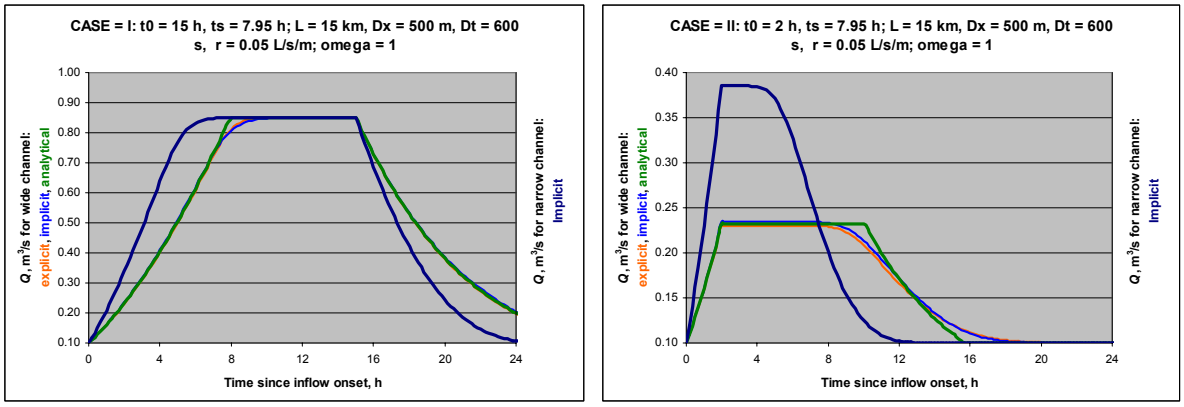

In Figure 3 we show predictions of the downstream hydrograph *Campylobacter* versus *E. coli*. In the former there is no sediment store ("s0" is the initial number of bacteria per unit area of sediment), but a constant concentration of *Campylobacter* in the lateral inflow (500 per 100 mL). In the latter case, there is both a lateral inflow concentration of *E. coli* and a substantial sediment concentration of that indicator.

Figure 3: Predicting differential timing of peaks of *Campylobacter* and *E. coli* concentrations, ignoring inactivation and using the explicit scheme.

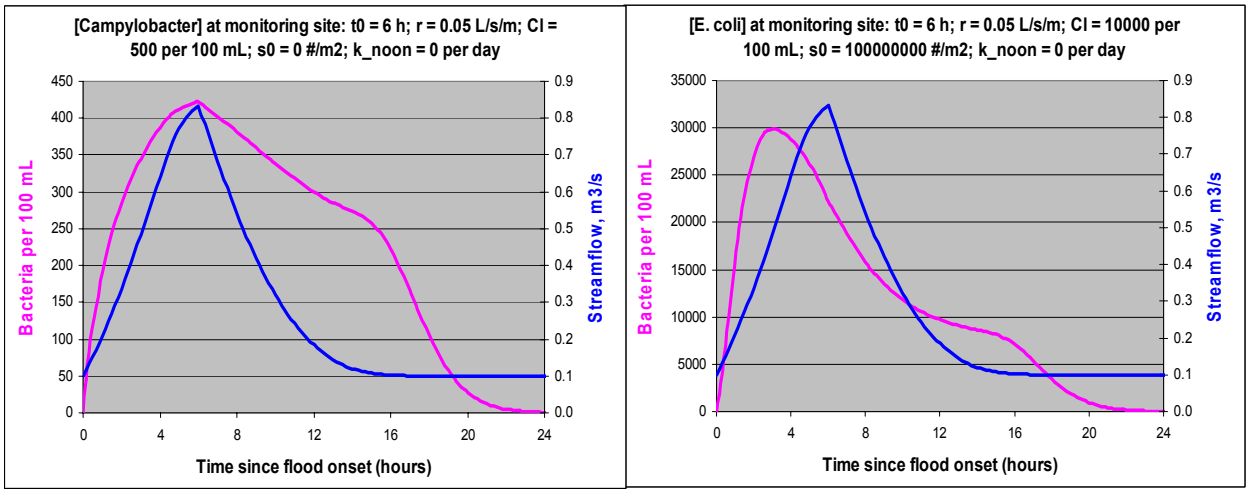

[5] As defined in the Appendix, t_s is the instant at which the stream discharge at the monitoring site first reaches its maximum possible value (for the given lateral inflow rate). In Case I ($t_0 > t_s$) the discharge remains at that value until the inflow ceases (at time t_0). In Case II ($t_0 < t_s$) the discharge remains at the value it attained at time t_0 for a subsequent time which we call the "recession overhang". That constant discharge value is always less than the maximum attained for Case I.

[6] "Omega" (ω) is the time-weight used in the four-point implicit scheme.

Figure 4: Predicting differential timing of peaks of *Campylobacter* and *E. coli* concentrations in the presence of inactivation, using the explicit scheme: *k* (per day) = 50 (*Campylobacter*), 10 (*E. coli*).

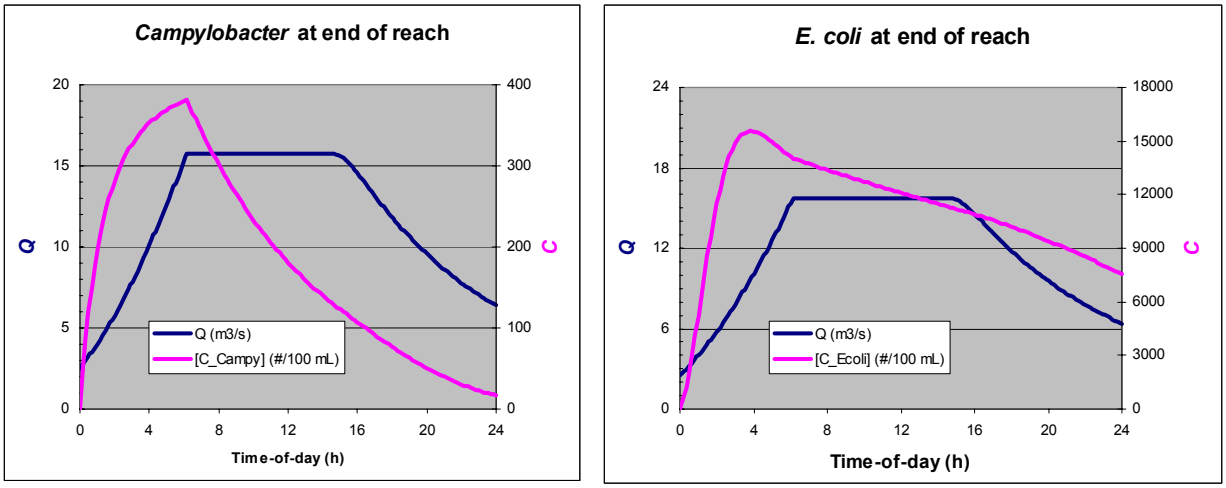

5. DISCUSSION AND CONCLUSION

The results in Figure 2 show that for the wide channel, the results predicted by both the explicit and implicit schemes agree well with the analytical solution. In fact the degree of agreement between the explicit and implicit schemes is surprising. However, mass conservation is not completely satisfactory for these calculations (there is a <0.5% error, and it should be smaller), a matter that awaits possible resolution.

Figure 3 demonstrates that the differential timing of peaks of *Campylobacter* and *E. coli* are able to be predicted by the model, merely by switching a sediment store off (for *Campylobacter*) and on (for *E. coli*). Figure 4 indicates that the same feature is predicted to occur even in the presence of (substantial) inactivation—field and laboratory studies show that the inactivation of *Campylobacter* under solar radiation is much faster than the equivalent rate for *E. coli* (Obiri-Danso *et al.* 2001, Sinton *et al.* 2007a&b).

This analysis indicates that *Campylobacter* may enter streams through storm runoff, rather than via sediment entrainment, and this could have important practical implications for the choice of effective Best Management Practices (BMPs) on farms, a topic of increasing interest in New Zealand—Collins *et al*. (2007), Lake *et al*. (2007), McBride & Chapra (in prep.). These results demonstrate the potential for simultaneous monitoring of indictors and pathogens, and associated kinematic wave modeling, to provide more informed understanding of the sources of the microbes that we are most interested in, yet seldom measure—the pathogens. Furthermore, the rapidly evolving field of microbial source tracking should provide even more discrimination on the differential infectivity pathogens according to their source. For example, *Campylobacter* from wild birds may be much less infective to humans than those originating from poultry, ruminant or human sources (French 2008).

ACKNOWLEDGEMENTS

This work was funded by the New Zealand Foundation for Research, Science and Technology via a contract with the New Zealand Food Safety Authority on the topic: "*Campylobacter* in food and the environment: establishing the link with public health". The writer also obtained a NIWA sabbatical grant in June-August 2009, during which time further work was performed on this topic. Drs Sharleen Harper and Chris Palliser have helped check details of the mathematical formulation.

REFERENCES

Abbott, M.B.; Basco, D.R. (1989). *Computational Fluid Dynamics: An Introduction for Engineers*. Longman/Wiley, New York.

Chapra, S.C. (1997). *Surface Water-Quality Modeling*. McGraw-Hill, New York.

Chow, V.T. (1959). *Open-Channel Hydraulics*. McGraw-Hill, New York

Collins, R.; McLeod, M.; Headley, M.; Donnison, A.; Close, M.; Hanly, J.; Horne, D.; Ross, C.; Davies-Colley, R.; Bagshaw, C.; Matthews, L. (2007). Best management practices to mitigate faecal contamination by livestock of New Zealand waters. *New Zealand Journal of Agricultural Research* **50**: 267–278.

Donnison, A.M.; Ross, C.M.; Davies-Colley, R.J. (2006). *Campylobacter* as indicated by faecal microbial contamination in two streams draining dairy country. Proceedings of the Water2006 conference, August 1–4, 2006, Hyatt Hotel, Auckland.

Eagleson, P.S. (1970). *Dynamic Hydrology*. McGraw-Hill, NY.

French, N.P. (2008). Enhancing surveillance of potentially foodborne enteric diseases in New Zealand: Human campylobacteriosis in the Manawatu. Final report **FDI / 236 /2005** to the New Zealand Food Safety Authority. Institute of Veterinary, Animal and Biomedical Sciences, College of Sciences Massey University, Palmerston North.[7]

Henderson, F.M. (1966). *Open Channel Flow*. Macmillan, London.

Henderson, F.M.; Wooding, R.A. (1964). Overland flow and groundwater flow from a steady rainfall of finite duration. *Journal of Geophysical Research* **69**(8): 1531–1540.

Krein, A.; De Sutter, R. (2001). Use of artificial flood events to demonstrate the invalidity of simple mixing models. *Hydrological Sciences Journal*. **46**(4), 611–622.

Lake, R.; van der Logt, P.; McBride, G.B.; French, N.P.; Mullner, P.; Elliott, A.H.; Ball, A. (2007). Campylobacteriosis in New Zealand: modelling as a way forward. *New Zealand Science Review* **64**(2): 37–41.

Li, R.-M.; Simons, D.B.; Stevens, M.A. (1975). Nonlinear kinematic wave approximation for water routing. *Water Resources Research* **11**(2): 245–252.

Liggett, J.A.; Cunge, J.A. (1975). Numerical methods of solution of the unsteady flow equations. Chapter 4 in: Mahmood, K. and Yevjevich, Y. (eds), *Unsteady Flow in Open Channels*, Volume 1, Water Resources Publications, Fort Collins, CO.

Lydiard, E.; Davies-Colley, R.J. (2006). Impact of rainstorms on faecal matter yields in pastoral waterways. NIWA Client Report HAM2006-13, 103 p.

Martin, J.L.; McCutcheon, R.W. (1999). *Hydrodynamics and Transport for Water Quality Modeling*. Lewis, Boca Raton.

McBride, G.B. (2009, in prep.). Kinematic wave and contaminant transport: revealing the sources.

McBride, G.B.; Chapra, S. (in prep.). New analytical model implies disproportionate reduction of zoonotic pathogens in watersheds after implementation of Best Management Practices on farms. For submission to *Water Research*.

McBride, G.B.; Mittinity, M. (2007). Explaining differential timing of peaks of a pathogen versus a faecal indicator during flood events. MODSIM07, Christchurch, December 10–13.

Muirhead, R.W.; Davies-Colley, R.J.; Donnison, A.M.; Nagels, J.W. (2004). Faecal bacteria yields in artificial flood events: quantifying in-stream stores. *Water Research* **38**: 1215–1224.

Nagels, J.W.; Davies-Colley, R.J.; Donnison, A.M.; Muirhead, R.W. (2002). Faecal contamination over flood events in a pastoral agricultural stream in New Zealand. *Water Science and Technology* **45**(12): 45–52.

Obiri-Danso, K.; Paul, N.; Jones, K. (2001). The effects of UBV and temperature on the survival of natural populations and pure cultures of *Campylobacter jejuni, Camp. coli, Camp. Lari* and urease-positive thermophilic campylobacters (UPTC) in surface waters. *Journal of Applied Microbiology* **90**: 256–267.

Rutherford, J.C. (1994). *River Mixing*. Wiley, New York.

Singh, V.P. (2002). Is hydrology kinematic? *Hydrological Processes* **16**: 667–716.

Sinton, L., Hall, C.; Braithwaite, R. (2007a). Sunlight inactivation of *Campylobacter jejuni* and *Salmonella enterica*, compared with *Escherichia coli* in sea water and river water. *Journal of Water and Health* **5**(3): 357–365.

Sinton, L.W.; Braithwaite, R.R.; Hall, C.H.; Mackenzie, M.L. (2007b). Survival of indicator and pathogenic bacteria in bovine faeces on pasture. *Applied and Environmental Microbiology* **73**(24): 7917–7925.

Snowsill, A. (2007). Faecal microbial contaminants in agricultural stream sediments, biofilm and vegetation. BSc (Technology) Industry Report BIOL370-07C, University of Waikato, Hamilton, New Zealand.

Streeter, V.L. (1966). *Fluid Mechanics*. 4th ed. McGraw-Hill, New York

Till, D.G.; McBride, G.B. (2004). Potential public health risk of *Campylobacter* and other zoonotic waterborne infections in New Zealand. Chapter 12 In: Cotruvo, J.A. *et al*. (eds), *Waterborne Zoonoses: Identification, Causes and Control*, IWA publishing, London, for the World Health Organization, pp. 191–207.

Valentine, E.M.; Wood, I.R. (1979). Experiments in longitudinal dispersion with dead zones. *Journal of the Hydraulics Division, American Society of Civil Engineers* **105**(HY12): 999–1016.

Wilkinson, J.; Kay, D.; Wyer, M.; Jenkins, A. (2006). Processes driving the episodic flux of faecal indicator organisms in streams impacting on recreational and shellfish harvesting waters. *Water Research* **40**: 153–161.

[7] http://www.nzfsa.govt.nz/science/research-projects/Campy_Attribution_Manawatu.pdf

NOMENCLATURE

Term[§]	Meaning	Generic units[†,¶]
α	Proportionality factor in the fundamental kinematic wave equation, $A = \alpha Q^{\beta}$	$L^{2-3\beta}\ T^{\beta}$
β	Exponent in the kinematic wave equation, $A = \alpha Q^{\beta}$ ($\beta = 3/5$ for Manning equation)	–
θ	Channel bed slope	–
μ	Relative stream water velocity excess, $\mu = (U - U_b)/U$	–
ρ	Units conversion factor in Manning equation, $Q = \rho[A^{5/3}\theta^{1/2}/(nP^{2/3})]$	$L^{2-1/\beta}\ T^{-1}$
A	Stream cross-section area	L^2
B_0	Stream width	L
C	Bacteria concentration in the stream water	$\#\ L^{-3}$
C_l	Bacteria concentration in the lateral inflow	$\#\ L^{-3}$
e_s	Stream sediment entrainment coefficient	T^{-1}
i	Distance counter for numerical scheme: $x = i\Delta x$	–
k	Bacteria inactivation coefficient	T^{-1}
L	Stream length from dam to downstream boundary	L
M_l	Delivery rate of land-derived bacteria per unit channel length	$\#\ T^{-1}\ L^{-1}$
M_s	Delivery rate of entrained bacteria per unit channel length	$\#\ T^{-1}\ L^{-1}$
n	Manning's "n", a resistance coefficient; also time step counter, $t = n\Delta t$	–
P	Stream channel wetted perimeter	L
Q	Stream rate of flow ("discharge")	$L^3\ T^{-1}$
Q_b	Stream discharge at baseflow	$L^3\ T^{-1}$
$Q_{\max,I}$	Maximum stream discharge at downstream boundary for Case I (see Appendix)	$L^3\ T^{-1}$
$Q_{\max,II}$	Maximum stream discharge at downstream boundary for Case II (see Appendix)	$L^3\ T^{-1}$
r	Lateral inflow rate per unit channel length	$L^2\ T^{-1}$
S	Store of sediments in stream sediments per unit channel length	$\#\ L^{-1}$
s	Store of sediments in stream sediments per unit bed area	$\#\ L^{-2}$
t	Time since commencement of lateral inflow	T
t_0	Duration of lateral inflow	T
t_s	Time of concentration, so that $Q = Q_{\max,I}$ for $t = t_s \le t_0$ (see Appendix)	T
t_p	Recession overhang for Case II (see Appendix)	T
t_{II}	Time at which Case II steady-state ceases (see Appendix)	T
t_{0s}	Time to (instantaneous) flood peak when $t_0 = t_s$ (see Appendix)	T
U	Cross-section-average water flow velocity	$L\ T^{-1}$
U_b	Cross-section-average water flow velocity at baseflow	$L\ T^{-1}$
U_c	Kinematic wave celerity	$L\ T^{-1}$
V	Steam segment volume, $V = A\Delta x$	L^3
X	Distance along the channel from the dam	L

[§] The lateral inflow term "r" is "q" in McBride & Mittinty (2007). The change has been made to avoid programming difficulties.

[†] "#" denotes numbers of bacteria; "L" denotes length; "T" denotes time.

[¶] The particular choice of units made must be such as to ensure dimensional consistency in the governing equations and in the associated computer code.

APPENDIX: ANALYTICAL FLOW SOLUTIONS FOR A WIDE CHANNEL WITH POSITIVE BASEFLOW

Henderson & Wooding (1964) developed an elegant analytical solution for an overland flow kinematic wave arising from steady rainfall of finite duration, given zero initial depth (see also Streeter 1966). This solution can be extended to the case of a lateral inflow of finite duration to a wide channel with positive baseflow (McBride, 2009 in prep.), providing an excellent "benchmark" for associated numerical solutions—at least for the flow component in a wide channel. The key equation is Eq. (5), i.e., $A = \alpha Q^{\beta}$ (with terms as defined previously).

First we must first define two key time periods: the duration of lateral inflow (t_0), and the time (t_s) at which a steady-state maximum flow is reached at the downstream boundary (at $x = L$). This time is also commonly called the catchment "time of concentration" (e.g., Eagelson 1970). It may be calculated as:

$$t_s = \frac{\alpha}{r}\left[(rL + Q_b)^{\beta} - Q_b^{\beta}\right] \tag{A.1}$$

where L is the length of the stream segment (from the dam to the downstream boundary), and all other terms are as defined previously (and are also listed in the immediately preceding Nomenclature section).

Following Henderson & Wooding (1964) we then define two cases—"Case I" and "Case II"—according to whether or not the lateral inflow duration exceeds the time of concentration (i.e., $t_0 > t_s$ or $t_0 < t_s$). Their associated water surface profiles are depicted on Figure A.1. In Case I, the profile **A'DC** will be attained after a time t_s. This will be maintained, with constant depth **BC** at the point **B**, until lateral inflow ceases (at the later time t_0). In Case II a water surface profile such **A'DE** will apply at time t_0, in which a plateau extends some way upstream of **B** with constant depth **BE** (less than **BC**). This depth will be maintained at **B** for some time *after* lateral inflow ceases, until a time t_{II}, which we can calculate. This time increment ($t_p = t_{II} - t_0$) we call the "recession overhang".

Figure A.1: Water surface profiles during the buildup and steady-state phases

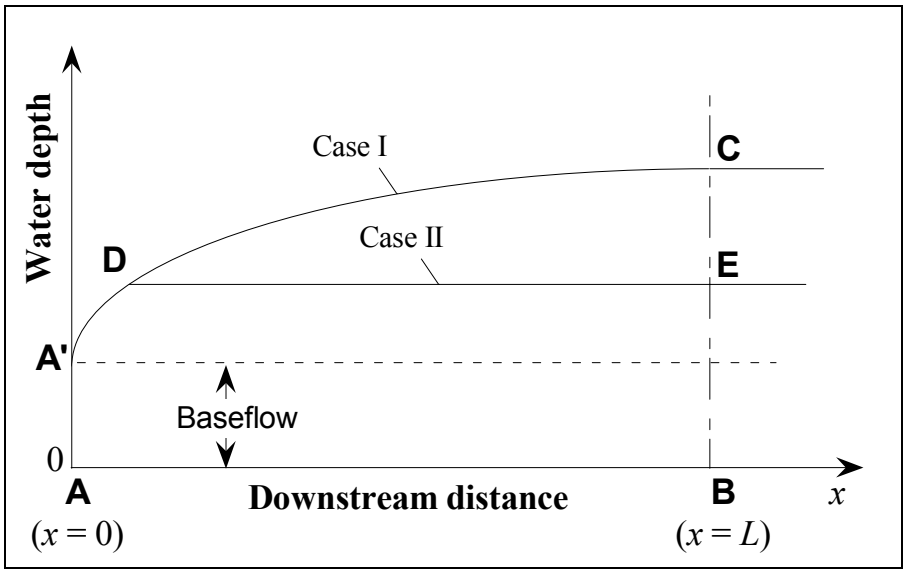

The analytical solutions for stream discharge are as follows:

$$\underline{\text{Case I}}\ (t_0 > t_s):\quad Q = \begin{cases} \left(\dfrac{rt}{\alpha} + Q_b^{\beta}\right)^{1/\beta} & : 0 < t \le t_s \\ Lr + Q_b \left(= Q_{\max,\mathrm{I}}\right) & : t_s < t \le t_0 \\ \begin{cases} Q_{\mathrm{rec,I}} & t < t_0 + L/U_{c,b} \\ Q_b & t \ge t_0 + L/U_{c,b} \end{cases} & : t > t_0 \end{cases} \tag{A.2}$$

where $U_{c,b} = Q_b^{1-\beta} / (\alpha\beta)$ is the celerity of the kinematic wave at baseflow (a known quantity), and

$$\underline{\text{Case II}}\ (t_0 \le t_s):\ Q = \begin{cases} \left(\dfrac{rt}{\alpha} + Q_b^{\beta}\right)^{1/\beta} & : 0 < t \le t_0 \\ \left(\dfrac{rt_0}{\alpha} + Q_b^{\beta}\right)^{1/\beta} \left(= Q_{\max,\mathrm{II}}\right) & : t_0 < t \le t_{\mathrm{II}} \\ \begin{cases} Q_{\mathrm{rec,II}} & t < t_0 + L/U_{c,b} \\ Q_b & t \ge t_0 + L/U_{c,b} \end{cases} & : t > t_{\mathrm{II}} \end{cases} \tag{A.3}$$

In each case the recession discharges ($Q_{\mathrm{rec,I}}$ & $Q_{\mathrm{rec,II}}$) are solutions of $f(Q) = L - [(Q - Q_b)/r + U_c(t - t_0)] = 0$, which is implicit in Q (because $U_c \propto Q^{1-\beta}$). This equation can be readily solved, to high accuracy, using the standard Newton-Raphson iterative method.

The time variable t_{II} in (A.3) is defined (for Case II only) as follows:

$t_{\mathrm{II}} = t_0 + t_p$ is the last time for which the flow at **B** remains constant ($= Q_{\max,\mathrm{II}}$)

where

$t_p = \beta(t_{0s} - t_0)$ is the afore-mentioned recession overhang, and

$t_{0s} = \alpha\left(Q_{\max,\mathrm{I}} Q_{\max,\mathrm{II}}^{\beta-1} - Q_b^{\beta}\right)/r$ is the time to the (instantaneous) peak discharge that occurs when the lateral inflow duration equals the time of concentration (i.e., $t_0 = t_s$), in which case Cases I and II coincide.